VOL. 12, NO. 23, DECEMBER 2017 ISSN 1819-6608
ARPN Journal of Engineering and Applied Sciences

www.arpnjournals.com

FEM MODELLING OF HUMAN EYE FOR INVESTIGATING THE THERMAL EFFECTS OF TUMOR ON THE OCULAR SURFACE TEMPERATURE

Sreethul Das[1] and Monica Subashini M.[2]
[1]School of Mechanical Engineering, VIT University, Vellore, India
[2]School of Electrical Engineering, VIT University, Vellore, India
E-Mail: monicasubashini.m@vit.ac.in

ABSTRACT

Choroidal Melanoma is a type of eye tumor found in the Choroidal tissue. Tumor has a very high metabolic activity which raises the temperature of the tissues in its surrounding. The heat generated by tumor would tend to increase the temperature on the corneal surface of eye. This resulting thermal asymmetry and increase in temperature maybe used in the detection of tumor. The proposed method aims to find out the variation in temperature distribution on cornea's surface due to the presence of tumor. A 3D eye model had been developed for this study. Tumors of various sizes are introduced at different locations in the eye model. The effects on the corneal temperature with reference to a normal eye have been studied. The results indicate that the presence of tumors T2, T3 (maximum in size) can be detected by the proposed method, whereas the temperature variation in the corneal surface produced by T1 tumor (least in size) is not significant enough to be detected. This analysis proved that thermal imaging of the human eye is a promising method in the detection of Choroidal melanoma compared to the existing diagnostic techniques.

Keywords: FEM simulation, eye tumor, ANSYS, ocular surface temperature.

1. INTRODUCTION

1.1 Background

A tumor is an abnormal growth of mass in any part of the body. The presence of such a mass inside (intraocular tumor) or around (extraocular tumor) the eye is an eye tumor. According to American Cancer Society, the major types of primary eye cancers found in adults are namely melanoma, lymphoma and Choroidal melanoma in middle aged adults [29]. Retinoblastoma and medulloepithelioma are the commonly found eye tumors in children [27].

Choroidal melanoma starts in the choroid or the ciliary body in almost 95 out of every 100 cases (95%) of eyeball melanoma. The other 5% begin in the iris [28]. It can cause vision losses due to detachment of retina. If this tumor is present near the eye lens, it can push the lens or change its configuration and shape leading to astigmatism. Other symptoms of choroidal melanoma include flashing lights or spots and severe pain in the eye.

Current methods to diagnose eye tumor include dilated eye exam, ultrasound, fluoresce in angiography and other imaging techniques [1]. Ultrasound technique uses high frequency sound waves to detect structural abnormalities in the part being tested. According to a report issued by National Council on Radiation Protection and Measurements Ultrasound [30], ultrasound is found to have thermal effects and mechanical effects on the body. These mechanical effects include movement of cells in liquid, electrical changes in cell membranes, shrinking and expansion of bubbles in liquid, and pressure changes. Fluorescein Angiography is a test in which a dye is used to observe the flow of blood in choroid and retina. There have been adverse reactions reported for this method, which include nausea, abdominal discomfort and rashes [2]. As discussed above, the diagnostic techniques currently in use have a few shortcomings and hence researchers have started working towards development of non-invasive methods. Current imaging techniques make it possible to research the potential applications of IR thermography as a reliable diagnostic tool eye disorders and other medical disorders.

B.B. Lahiri *et al*, [21] discusses the applications of IR thermography as a non-invasive diagnostic technique. E.Y.-K. Ng [22] has evaluated the capabilities and limitations of IR imaging for medical diagnosis and has detailed the procedure and instrumentation associated with its application for detection of breast cancer. Tan [23] has reviewed the applications of IR thermography for detection of ocular diseases based on ocular surface temperature obtained from the thermal imaging.Acharya, U. Rajendra *et al* [24] has developed an automated method for detecting dry eye disorder using IR thermal imaging. They have proposed their method as a diagnostic tool for ophthalmologists for faster detection of ocular abnormalities during mass screening. These studies indicate that IR thermography can be developed as a reliable method for detecting ocular abnormalities.

Normal eye temperature distribution has been simulated and atmospheric effects on human eye have been determined by Firoozan *et al* [3] in their studies. They have developed a finite element model for the same. In the study carried out by E.H. Ooi∗, W.T. Ang, E.Y.K.Ng [4] a numerical boundary value model of the eye was developed considering the effects of thermal conductivity, blood perfusion and metabolic heat generations. Their studies demonstrate that thermal effects of tumor can be simulated accurately using mathematical models. The rise in temperature and thermal asymmetry generated by the tumor are potential indicators of presence

of tumor. The objective of the proposed method b is to refine their technique by studying the combined effect of tumor size, location and thermal properties of tumor on the corneal surface temperature. The outcome of the current study indicates the feasibility of using the proposed technique in the diagnostic procedure. Tumors of different sizes are introduced at different locations in the human eye and the resulting temperature distribution on the corneal surface has been obtained using ANSYS and SOLIDWORKS [31] software. The temperature profiles thus obtained on corneal surface of tumorous eye are then compared with that of a normal human eye to confirm the presence of tumor.

2. METHODOLOGY

2.1 Modelling of eye

The human eye has been modeled in to five major regions namely cornea, aqueous humor, lens, vitreous humor and sclera using the dimensions in Table-1.

Table-1. Dimensions used for modelling of eye.

Part name	**Dimension** (mm)	**Reference**
Cornea		
Thickness	0.5	[7], [8]
Outer radius	7.89	[8]
Inner Radius	6.7	[8]
Aqueous humor		
Thickness	3.05	[9]
Vitreous humor		
horizontal extension at lens	16.4	[9]
Sclera		
Thickness	0.5	[11]
Radius	11.5	[13]
Pupil		
Diameter	3	[12]
Lens		
Thickness	4.2	[8], [10]
Anterior Radius of Curvature	11	[8]
Posterior Radius of Curvature	6	[8]

The thermal properties of iris are similar to those of sclera and hence they are modeled together as one region [6]. Choroid and retina have been considered with sclera because of their relatively negligible thickness [17]. Optic nerve has not been included in the overall geometry since its effect on the ocular thermal distribution is not significant [17]. The 2D sketch of the eye developed using SOLID WORKS is shown in Figure-1.

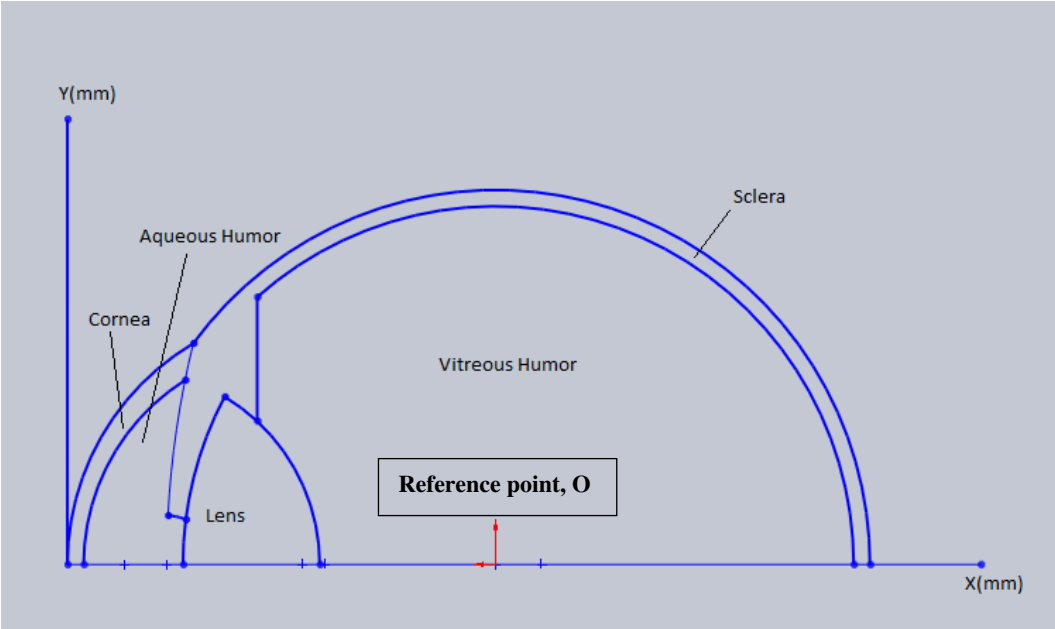

Figure-1. 2D-Model of eye developed using SOLIDWORKS showing major regions. The x- axis corresponds to the pupillary axis of the eye. Point O is used as the reference to specify the tumor locations.

The type of eye tumor considered in this method is Choroidal Melanoma. It is the most common type of eye cancer generally affecting people belonging to the age group 40-60 years [[2]NCBI]. According to researchers [14, 15], the tumorsare dome shaped or mushroom shaped, the dome shaped tumor being the more common one [16]. The [3]UICC, classifies choroidal melanoma using three parameters being size (T), number of lymph nodes (N) and metastatis's presence (M). As per the sixth edition of TNM classification, TNM6, choroidal melanoma can be grouped into four categories namely T1, T2, T3 and T4. These categories vary from each other on the basis of the [1]LBD and the thickness (t) of the tumor. The thickness here refers to apical height of tumor from its base. To study the effects of tumor, 2D models of T1, T2 and T3 tumors have been embedded at three locations in the eyeball. The other dimensions used for modelling the tumor types are shown in Table-2 and are within the recommended range.

Table-2. Criteria for choroidal melanoma classification based on T category of TNM6 [4]

Category	Description			
	LBD* (defined range) in mm	LBD (used) in mm	t** (defined range) in mm	t (used) in mm
T1	≤10	5.00	≤2.5	2.5
T2	≤15	10.00	≤5	5
T3	>15	15.00	>5	7.5
T4	Tumor extends beyond the eyeball			

*LBD: Largest Basal Diameter; **t: tumor thickness

2.2 Modelling assumptions

The size of human eye varies between 23 mm to 25mm in diameter with individual and age. An average size of 24.65mm has been considered for modelling the eye. The average value of sclera thickness is considered to be uniform as opposed to varying it at different locations. Also, thickness of lens is taken to be a constant of 4 mm though it keeps varying with age and distance of object under observation. For the purpose of analysis, the human eye is divided into 5 different regions based on the similarities in properties. The properties of various regions of human eye are given in Table-3.

Table-3. Properties of major regions [5]

Region	**Specific heat** (J kg $^{-1}$K^{-1})	**Thermal conductivity** (Wm^{-1}K^{-1})	**Density** (kgm^{-3})
Cornea	4178	0.58	1050
Lens	3000	0.4	1050
Aqueous Humor	3997	0.58	996
Vitreous Humor	4178	0.603	1000
Sclera	3180	1.0042	1100
Tumor		0.35-0.67	

2.3 Simulation in ANSYS

Although tumors are heterogeneous in nature, we have assumed the tumors T1, T2 and T3 to be homogeneous in nature. The effect of blood perfusion rate on the temperature distribution in the eye was reported to be minimal according to E.H. Ooi *et al* [1]. The current study has also ignored its effect on the corneal temperature distribution. The tumor has been placed at three probable locations (0° to 90° with reference to chosen point 'O') in the eyeball to simulate its effect on the corneal surface temperature. At each location, for a given type of tumor, simulations are carried out by varying the thermal conductivity and metabolic heat generation rate. The finite element model was discretized using the in-built meshing tool in ANSYS. The thermal boundary conditions and the parameters used for the simulation are given in Table-4 and Table-5.

Table-4. Thermal boundary conditions used in the analysis [4]

Parameter	**Value**
Ambient convection coefficient(Wm^{-2} K^{-1})	10
Blood convection coefficient(Wm^{-2} K^{-1})	65
Ambient temperature (K)	298
Blood temperature (K)	310
Tears evaporationrate(Wm^{-2})	40
Corneal surface emissivity	0.975
Tumor metabolic heat generation(Wm^{-3})	15,000-80,000

Table-5. Parameters varied in simulations

Location of tumor [Fig4-6]	**Size of tumor [Table3]**	**Thermal conductivity of tumor** (W/(m. K) **[4]**	**Heat generation of the tumor** (Wm^{-3}) **[4]**
L1(0 degrees)	T1	0.35	40,000
L2(45 degrees)	T2	0.45	60,000
L3(90 degrees)	T3	0.55	80,000

The simulation is performed for the other tumor types and at the chosen locations. A total of 81 simulations resulted for the chosen combination of parameters. Temperature distribution of the normal eye has also been simulated for the purpose of comparison [31]. The 2D models of eye with the tumor embedded in the eyeball are shown in Figure-2 (a-c).

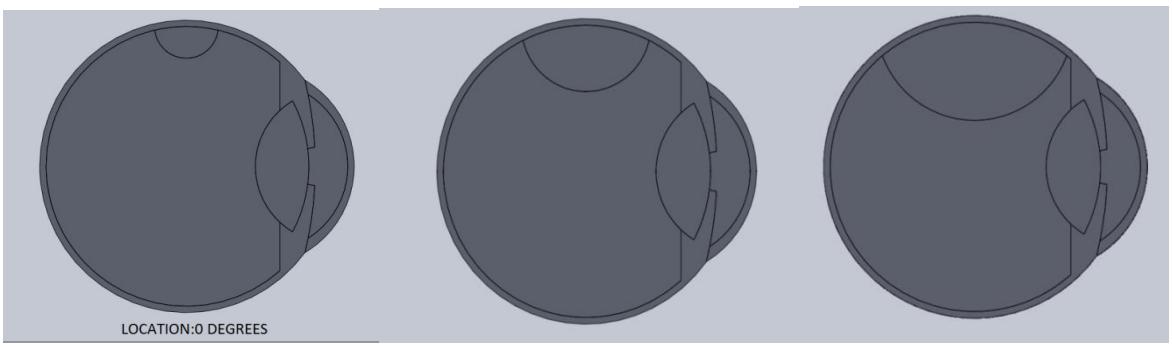

2(a) 2(b) 2(c)

Figure-2. (a)Represents the tumor T1, (b) represents the tumor T2 and (c) represents the tumor T3. The location of these tumors implanted is at 0°.

T4 tumor is not considered in this study as it extends beyond the eye ball. The most probable occurrence of choroidal melanoma is at the region shown in Figure-3(a).

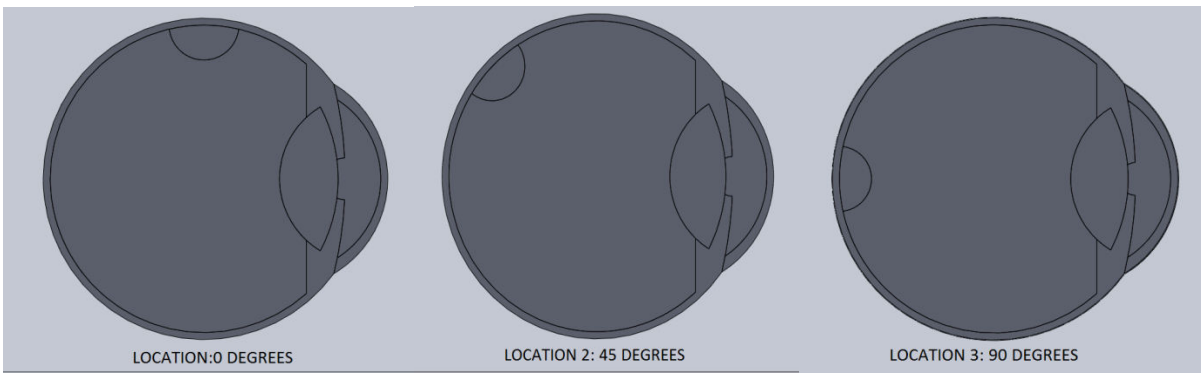

3(a) 3(b) 3(c)

Figure-3(a-c). Represents the location of tumor present in the modelled eye at 0°, 45° and 90° respectively with respect to the reference point O.

Here the choroid is the thickest and serves best place to form tumor. Figures 3(b) and 3(c) shows the other locations chosen to study the effects of eye tumor on the corneal surface temperature. To investigate the presence of tumor and its thermal effects on corneal surface, 28 nodal points on the corneal arc Z, as depicted in Figure-4, are taken into account.

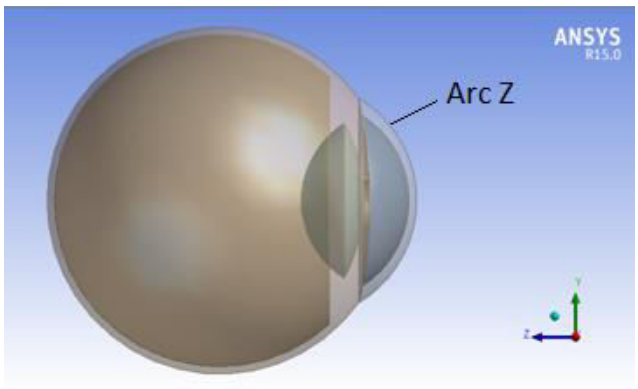

Figure-4. Normal eye depicting arc Z as seen from the plane perpendicular to the pupillary axis.

Each node is at an approximate distance of 0.588mm from each other. After the simulation, temperature at each node located on the corneal arc Z is measured for obtaining the corneal temperature distribution. The temperature on the nodes is plotted for the tumourous eye at locations L1, L2 and L3 and compared with that of the normal eye once the simulations are completed. For each location, a graph for the maximum temperature deviation of the corneal surface for a tumorous eye from the normal eye is made for the chosen combination of parameters.

3. RESULT ANALYSIS

3.1 Corneal surface temperature

Tan *et al* [25] has performed a statistical study on 67 test subjects to obtain the ocular surface temperature (OST) of a normal eye and the average OST calculated was 34.01 ± 0.64°C. A similar study was performed by Tkacova *et al* [20] and has reported the overall average temperature of the normal eye surface to be 34.51 ± 0.82°C. This value would serve as a reference for comparison with thermogram for identifying ocular abnormalities. The corneal surface temperature of normal eye simulated in the proposed method also falls in this

referred range. Further the temperature profile plotted along the pupillary axis for the normal eye is also similar to that reported by Tan *et al* [19, 26]. This validates the methodology followed in the current study for simulating the corneal surface temperature.

Analysis of results obtained from the simulations indicates that the presence of tumor in the eye alters the corneal surface temperature distribution. Figure-5(a-i) shows the temperature at the nodal

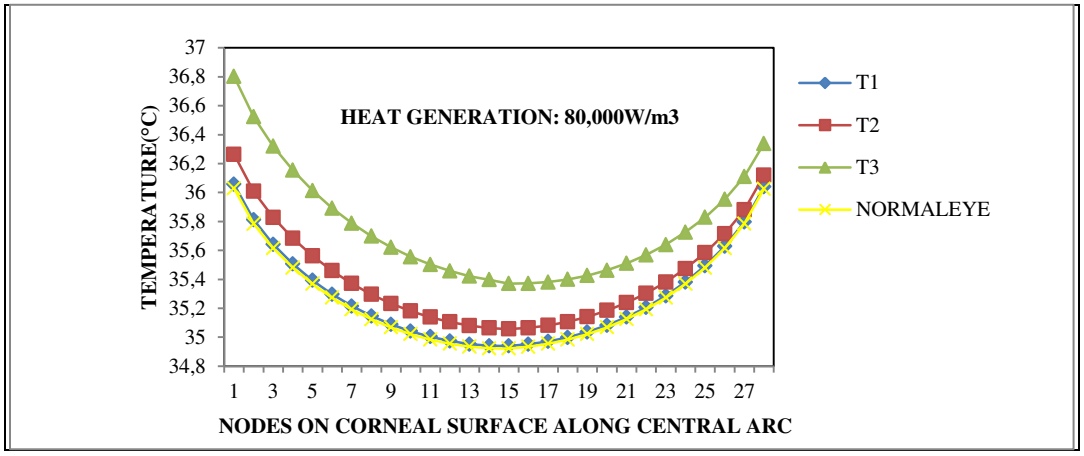

5(a)

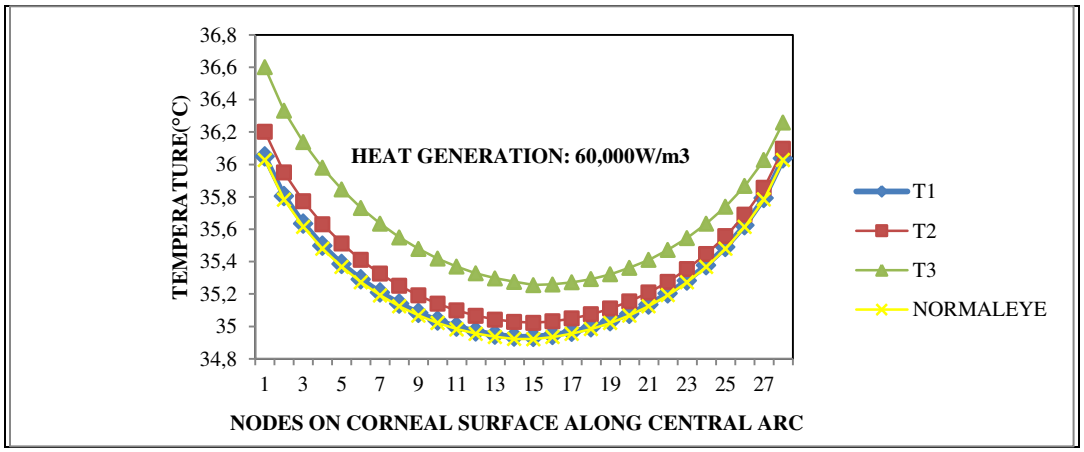

5(b)

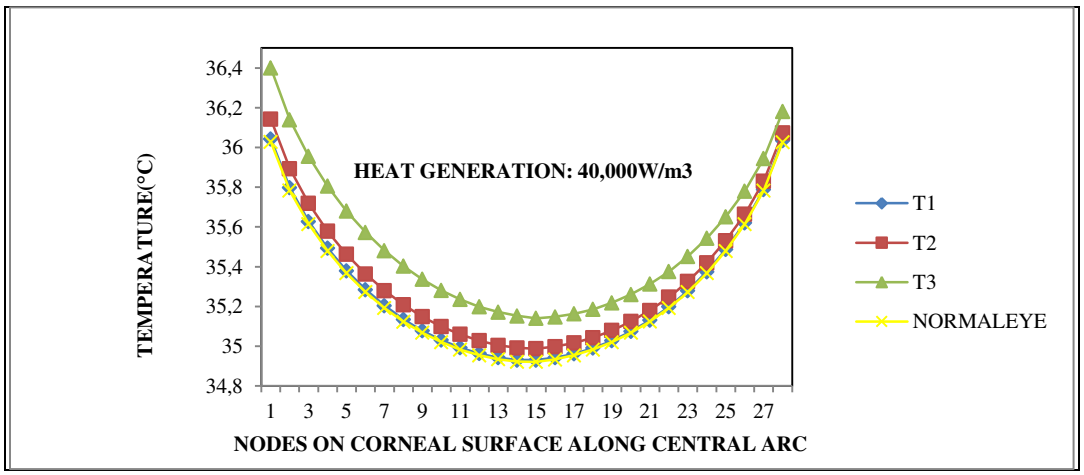

5(c)

Figure-5(a), (b), (c). Represents the comparison of corneal temperature distribution along arc Z for different tumor grades with that of a normal eye for k = 0.35 W/mK and Location L1 at various heat generation rates.

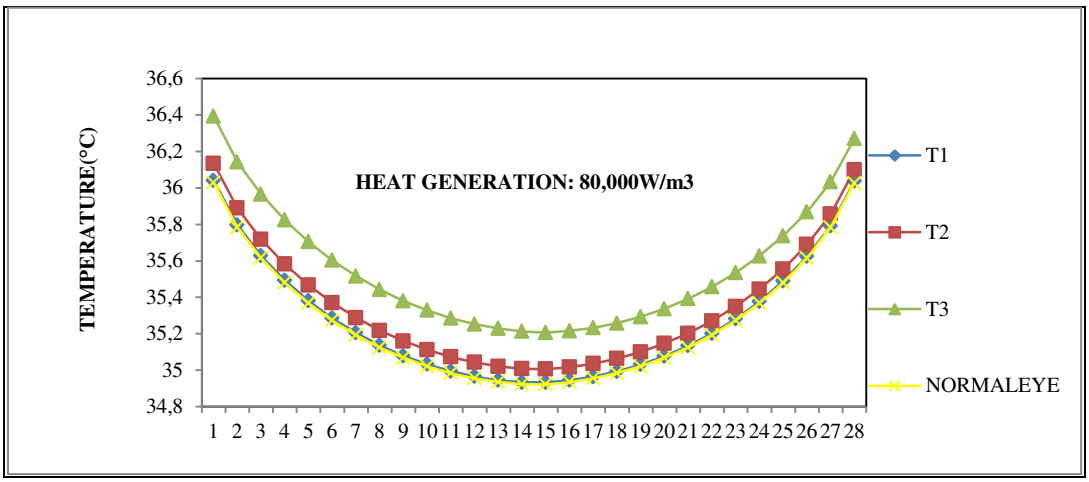

5(d)

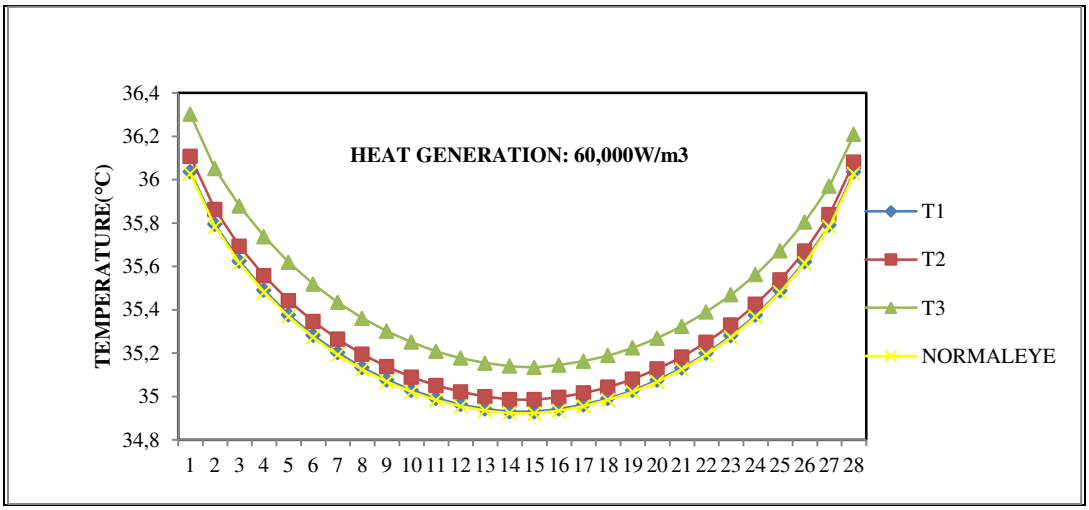

5(e)

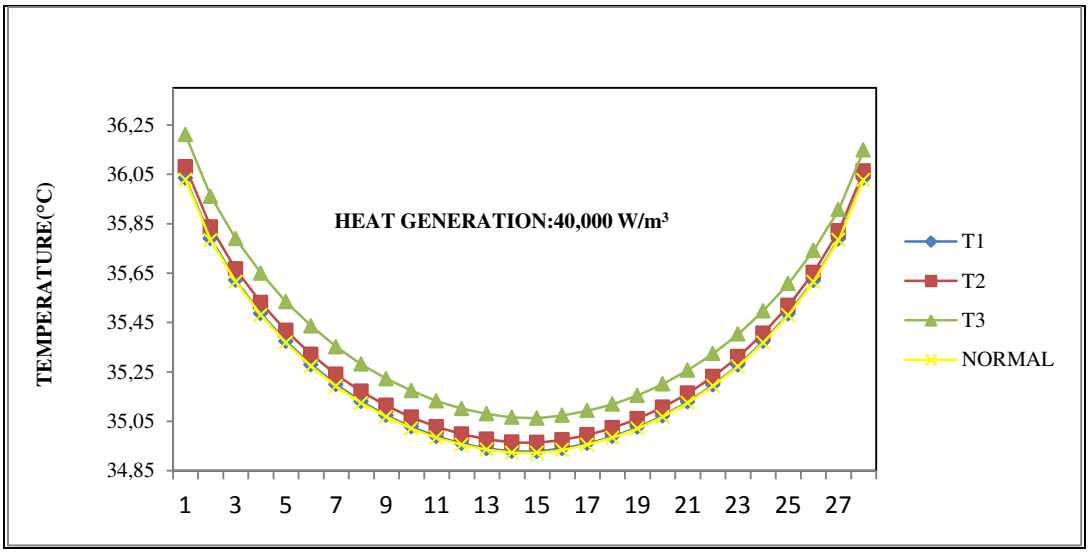

5(f)

Figure-5(d), (e), (f). Depicts the comparison of corneal temperature distribution along arc Z for different tumor grades with that of a normal eye for k = 0.35 W/mK and Location L2 at various heat generation rates.

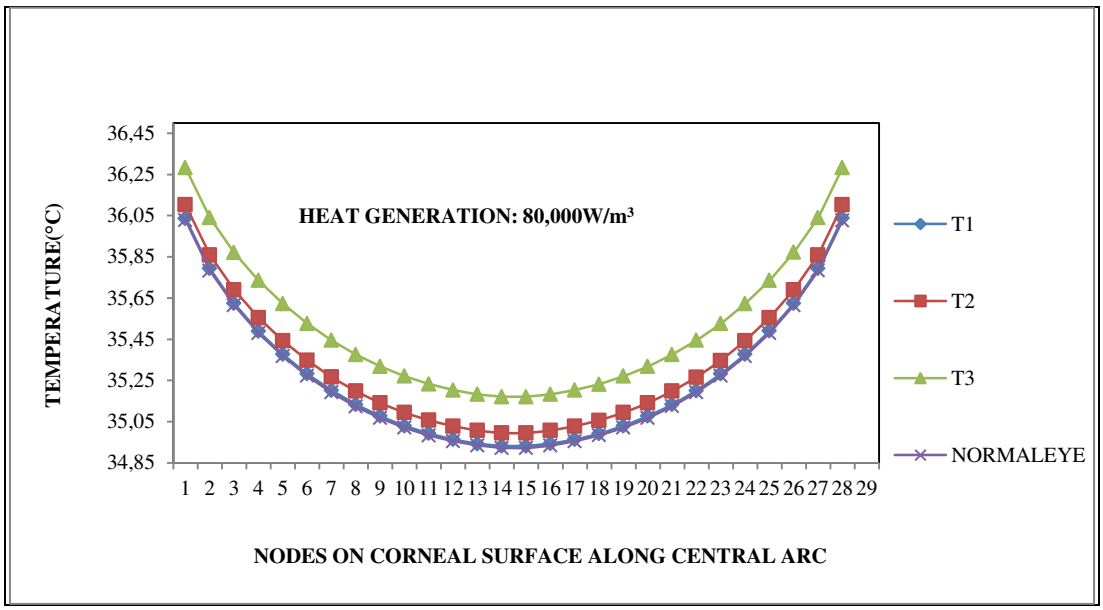

5(g)

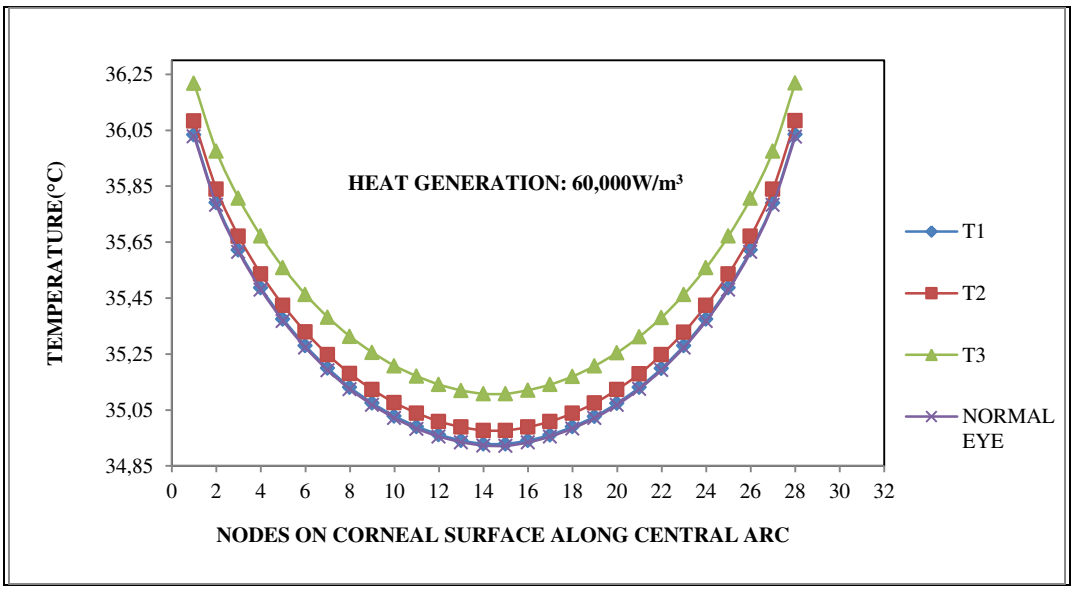

5(h)

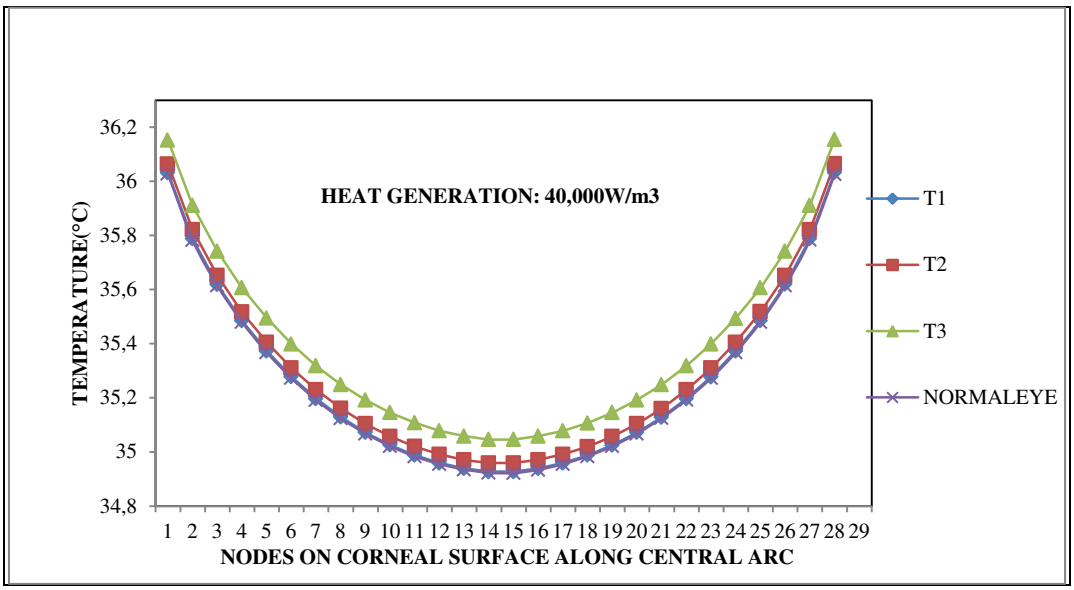

5(i)

Figure-5(g), (h), (i). Depicts the comparison of corneal temperature distribution along arc Z for different tumor grades with that of a normal eye for k = 0.35 W/mK and Location L3 at various heat generation rates.

points along arc Z of a tumorous eye, for the tumor grades considered with different rates of heat generation (thermal conductivity, k = 0.35 W/mK). The temperature profiles for other values of thermal conductivities, k= 0.45 W/mK & k=0.55 W/mK) have also been obtained. Temperature distribution for normal eye has been studied and considered for validation. The corneal temperature for a tumorous eye is higher than that of the normal eye. Further it can be seen that for a tumorous eye there is an asymmetry in the temperature distribution along the arc Z. E. H. Ooi *et al* [4] has studied the effects of tumor size, metabolic heat generation rate, thermal conductivity and blood perfusion rate on corneal surface temperature. Their results show that variation in corneal temperature distribution may indicate the presence of tumor. The result obtained by the proposed analysis confirms their observation.

3.1.1 Effect of tumor size and heat generation

The maximum temperature deviation of corneal surface of a tumorous eye increases with tumor size and it is observed from Figures 7 (a - c) for a given location and metabolic heat generation rate. As expected the temperature deviation increases proportionately with metabolic heat generation rate for a given tumor size.

3.1.2 Effect of tumor location

The temperature effects at location L1 for different metabolic heat generation rates of the tumor are depicted in Figures 5(a-c). The plots clearly indicate that for a given location, the corneal temperature deviates more from the normal eye for a higher tumor size and larger metabolic heat generation rate. Figures 5(d-f) and 5(g-i) shows the corneal temperature distribution at locations L2 and L3 respectively. By comparing the plots corresponding to L1, L2 and L3 it can be concluded that for a given tumor size, closer the tumor is to cornea, higher is the temperature deviation from the normal eye and greater is the asymmetry in temperature distribution. Hence tumors closer to cornea can be detected. The thermal asymmetry is observed as a shift in temperature bands as shown in Figures (6a) and (6b), which differentiates the tumorous eye from a normal eye.

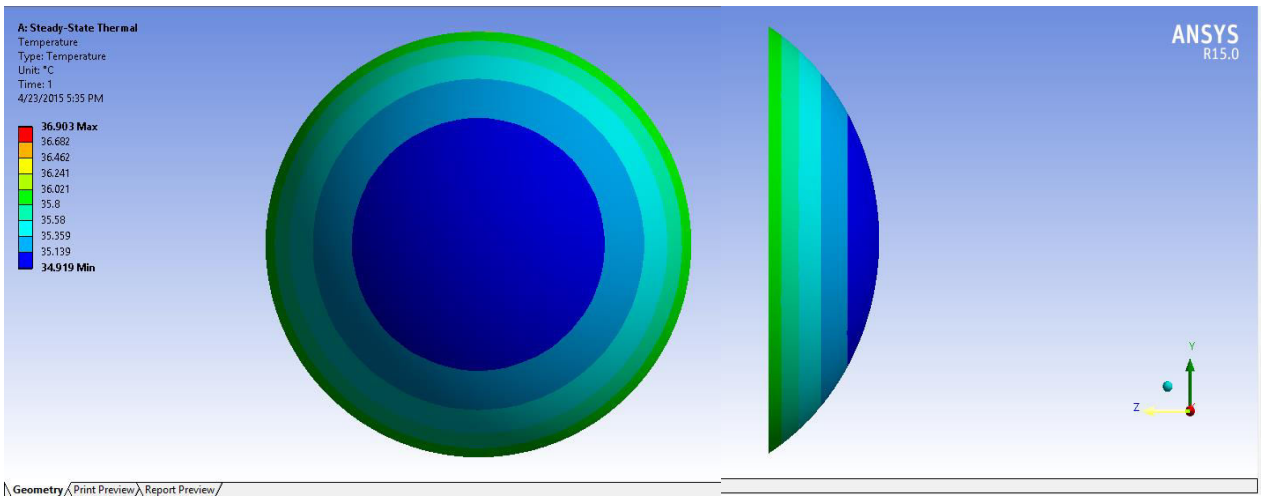

Figure-6(a). Temperature distribution of corneal surface of a normal eye.

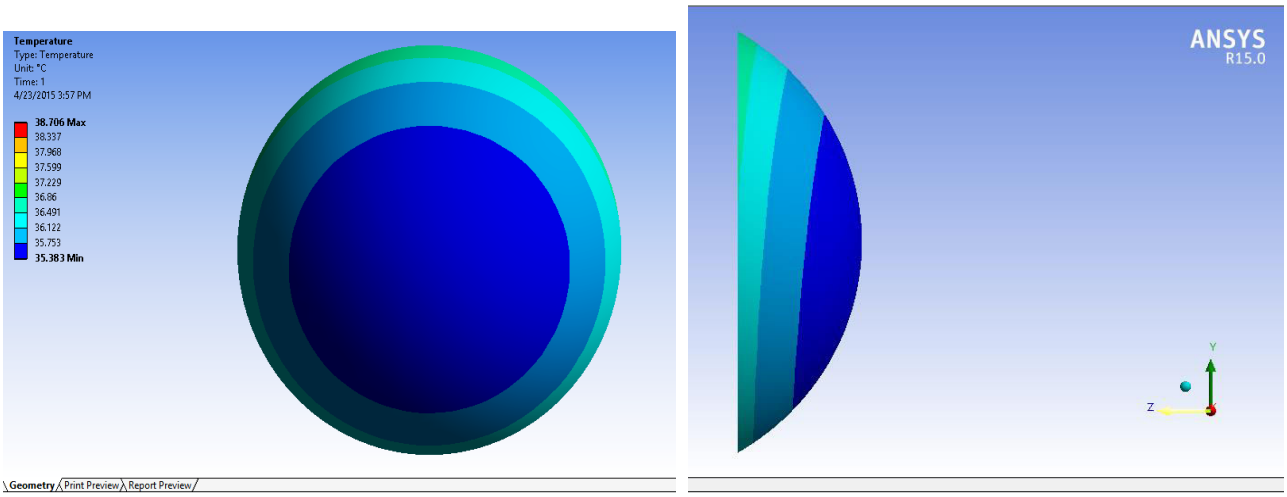

Figure-6(b). Temperature distribution of the corneal surface of a tumorous eye for tumor size T3, at L1 for thermal conductivity0.55Wm^{-1}K^{-1} and heat generation 80,000W/m^3.

3.1.3 Effect of thermal conductivity

The maximum temperature deviation of the tumorous eye with respect to the locations L1, L2 and L3, thermal conductivity values 0.35, 0.45 and 0.55 Wm^{-1}K^{-1} and heat generation rates40000, 60000 and 80000 W/m^3 has been plotted for various tumor sizes Figures (7a-7c). It is observed that for a given tumor size and metabolic heat generation rate, the maximum deviation of temperature remains almost a constant for the chosen values of thermal conductivity. Hence it can be inferred that for a given tumor size and heat generation rate, the maximum temperature deviation is not affected by thermal conductivity.

ARPN Journal of Engineering and Applied Sciences

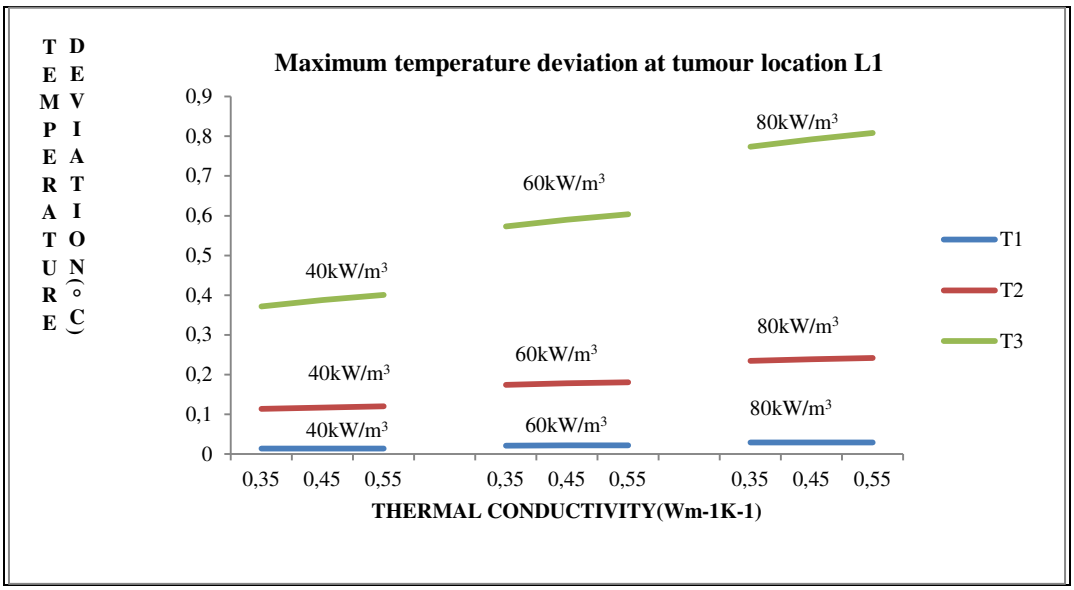

Figure-7(a). Thermal conductivity effects at L1 for various tumor sizes and heat generation rates.

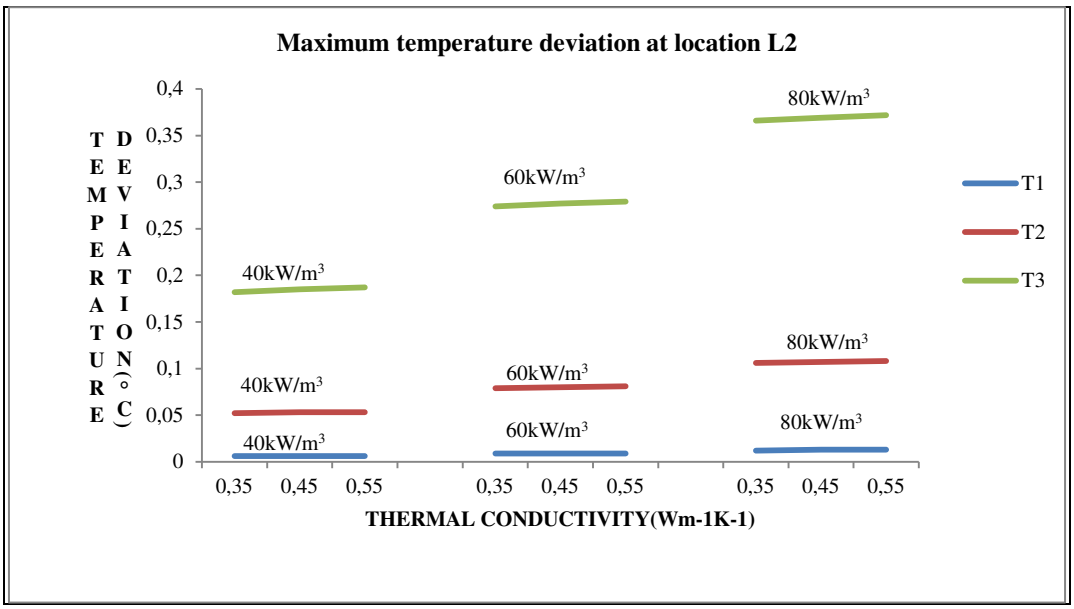

Figure-7(b). Thermal conductivity effects at L2 for various tumor sizes and heat generation rates.

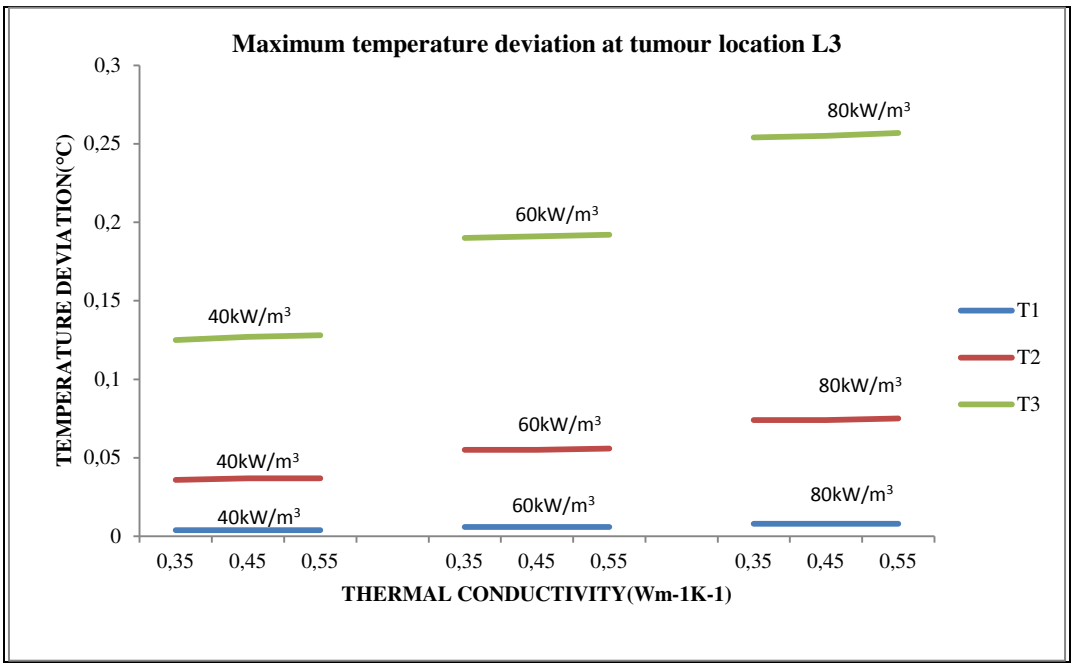

Figure-7(c). Thermal Conductivity effects at L3 for various tumor sizes and heat generation rates. The plot clearly shows that the maximum deviation of corneal surface temperature of a tumorous eye from the normal eye is increases with the tumor size and metabolic heat generation rate whereas the effect of varying the thermal conductivity is negligible.

DISCUSSIONS

The above analysis resulted from simulations indicate that the presence of tumor causes a change in temperature of the eyeball, which can be measured at the corneal surface. Hence it can be concluded that the change in temperature of the corneal surface may indicate the presence of tumor. Tumor size (T1, T2, T3), tumor location relative to the cornea (L1, L2, L3) and metabolic heat generation rate are the major factors that cause the change in corneal surface temperature and asymmetry in temperature distribution. The presence of tumor results in an asymmetrical temperature distribution at the cornea. The closer the tumor is to cornea, the higher is the observed rise in temperature and the asymmetry. This thermal asymmetry differentiates the tumorous eye from a normal eye. The probable location of the tumor can be found out from the asymmetry of temperature distribution. The maximum thermal asymmetry and rise in temperature (0.808 ^{o}C) with respect to that of the normal eye is observed for T3 size tumor with a heat generation rate of 80000 W/m^3 at location L1 (Figure-7a). The temperature deviation and asymmetry in temperature distribution are prominent for T3 and T2 tumors and hence the larger tumors inside the eye can be diagnosed using the proposed method. The temperature profile on the corneal surface due to T1 is almost similar to that of the normal eye, even at location L1, making it difficult to diagnose.

CONCLUSIONS

The objective of the proposed technique is to develop a non-invasive method for the detection of choroidal melanoma by measuring the corneal surface temperature. For this, a three dimensional symmetrical model of human eye has been developed to investigate the effect of tumor on the temperature distribution of corneal surface. From the results it has been observed that the temperature distribution of the tumorous eye depends on tumor size, location and tumor metabolism, thereby indicating that the variation in corneal surface temperature can be used for the diagnosis of tumor. So a larger tumor with higher metabolism closer to the cornea has more probability of being detected from the proposed method. The results obtained are in good agreement with the existing works and numerical solutions. Thus far, the usage of IR thermograph has been limited only to breast and skin cancer detection. The results obtained from the current study indicate a direct correlation between the temperature distribution of the corneal surface and the presence of tumor in the eye. Hence the study focuses towards the possibility of using IR thermography for developing a non-invasive method for the diagnosis of choroidal melanoma. Further research should be directed towards establishing a standard procedure and the required instrumentation for developing a diagnostic tool and validation of the method by clinical trials.

ACKNOWLEDGEMENT

We render our sincere thanks to the management, VIT University for providing us the necessary resources and support for completing the project.

REFERENCES

[1] Parul Singh, Abhishek Singh. 2012. Choroidal melanoma. Oman journal of ophthalmology. 5(1): 3-9.

[2] Musa F, Muen WJ, Hancock R, Clark D. 2006. Adverse effects of fluorescein angiography in hypertensive and elderly patients. Acta Ophthalmol Scand. 84(6).

[3] Mohammad Sadegh Firoozan, Soheil Porkhial n, Ali Salmani Nejad. 2014. Effect of tissue and atmosphere's parameters on human eye temperature distribution. Journal of Thermal Biology. p. 47.

[4] E.H. Ooi, W.T. Ang, E.Y. K.Ng. 2009. A boundary element model for investigating the effects of eye tumor on the temperature distribution inside the human eye, Computers in Biology and Medicine. 39(8): 667-677.

[5] E.Y.K. Ng, E.H. Ooi. 2006. FEM simulation of the eye structure with bioheat analysis. Computer Methods and Programs in Biomedicine. 82(3): 268-276.

[6] U. Cicekli. 2003. Computational model for heat transfer in the human eye using the finite element method, M.Sc. Thesis. Department of Civil and Environmental Engineering, Louisiana State University.

[7] Panagiotis A. Tsonis. 2008. Animal Models in Eye Research. Academic Press, San Diego, CA, USA.

[8] Wilson C N. 2011. A fully customizable anatomically correct model of crystalline lens, Ph. D Thesis, Department of Physics, University of Ottawa.

[9] Nico Heussner; Lukas Holl; Ariana Shults; Thorsten Beuth; Harsha Umesh Babu; Leilei Shinohara; Siegwart Bogatscher. 2013. Matthias Wippler; Wilhelm Stork Thermodynamic Finite-Element-Method (FEM) eye model for laser safety considerations, Proc. SPIE 8579, Optical Interactions with Tissue and Cells XXIV, 85790J.

[10] Wiley-VCH. 2008. Handbook of Optical Systems: Vol. 4 Survey of Optical Instruments.

[11] Richard E Norman, John G Flanagan, Sophie M K Rausch, Ian A Sigal, Inka Tertinegg, Armin Eilaghi, Sharon Portnoy, John G Sled, C Ross Ethier, Dimensions of the human sclera: Thickness measurement and regional changes with axial length, Experimental Eye Research. 90(2): 277-284, 2010.

[12] Somying Thainimit, Luís A. Alexandre, Vasco M. N. de Almeida. 2013. Iris Surface Deformation and Normalization. 13th International Symposium on Communications and Information Technologies (ISCIT). pp. 501-506.

[13] Peter G Watson. 2012. The Sclera and Systemic Disorders, 3/e edition, 352.

[14] J.M. Romero, P.T. Finger, R.B. Rosen, R. Iezzi. 2001. Three-dimensional ultrasound for the measurement of choroidal melanoma, Arch. Ophthalmol. 119(9): 1275-1282.

[15] I. Kaiserman, R. Amer, N. Kaiserman, J. Pe'er. 2005. Ultrasonographic tissue characteristics of mushroom-shaped uveal melanoma, Curr. Eye Res. 30(3): 171-177.

[16] 2006. Bruch's membrane abnormalities in dome-shaped and mushroom-shaped choroidal melanomas. Hainsworth DP, Sommerville DN, Ranson NT, Todd KC, Gigantelli JW.Ann Acad Med Singapore. 35(2).

[17] E.H. Ooi, W.T. Ang, E.Y.K. Ng. 2007. Bioheat transfer in the human eye: a boundary element approach, Eng. Anal. Boundary Elem. 31(6): 494-500.

[18] M. Gautherie. 1980. Thermopathology of breast cancer: measurement and analysis of in vivo temperature and blood flow, in: R. Jain, P. Gullino (Eds.), Thermal Characteristics of Tumor: Applications in Detection and Treatment, Ann. N. Y. Acad. Sci. 335: 383-415.

[19] Jen-Hong Tan, E.Y.K. Ng, Rajendra Acharya. 2008. Detection of eye and cornea on IR thermogram using genetic snake ALGORITHM. 9th International Conference on Quantitative Infra Red Thermography, July 2-5, Krakow - Poland (Intro)

[20] M. Tkacova, J. Zivcak, P. Foffova. 2011. A Reference for Human Eye Surface Temperature Measurements in Diagnostic Process of Ophthalmologic Diseases, MEASUREMENT 2011, Proceedings of the 8th International Conference, Smolenice, Slovakia. (meth)

[21] B.B. Lahiri, S. Bagavathiappan, T. Jayakumar, John Philip. 2012. Medical applications of infrared thermography: A review, Infrared Physics & Technology. 55: 221-235.

[22] Ng E.Y.K. 2009. A review of thermography as promising non-invasive detection modality for breast

tumor: International Journal of Thermal Sciences. 48: 849-859.

[23] Tan Jen-Hong; Ng E. Y. K.; Rajendra Acharya U.; Chee C. 2009. Infrared thermography on ocular surface temperature: A review, Infrared Physics & Technology. 52: 97-108.

[24] Acharya U. Rajendra; Tan Jen Hong; Koh Joel E. W.; Sudarshan Vidya K.; Yeo Sharon; Too Cheah Loon; Chua Chua Kuang; Ng E. Y. K.; Tong Louis. 2015. Automated diagnosis of dry eye using infrared thermography images. Infrared Physics& Technology. 71: 263-271.

[25] Jen-Hong Tan, E.Y.K. Ng, Rajendra Acharya U, C. Chee. 2010. Automated study of ocular thermal images: Comprehensive analysis of corneal health with different age group subjects and validation, Digital Signal Processing. 20: 1579-1591.

[26] Jen Hong Tan, E.Y.K. Ng, U. Rajendra Acharya. 2011. Evaluation of topographical variation in ocular surface temperature by functional infrared thermography. Infrared Physics & Technology. 54, 469-477.

[27] http://www.cancer.org/cancer/eyecancer/detailedguide/eye-cancer-what-is-eye-cancer.

[28] http://www.cancerresearchuk.org/about-cancer/type/eye-cancer/about/types-of-eye-cancer.

[29] http://www.isoo.org/melanoma.

[30] http://www.ncrponline.org/Publications/Reports/Misc_PDFs/Ultrasound%20Summary--NCRP.pdf.

[31] 2015. B. Tech Thesis: Darshna Sharma, Ashwini Ulhas Bhangale, Monica Subashini. M, 3D Modelling and Simulation of human eye to investigate the presence of Choroidal melanoma and its effects on the corneal surface temperature. School of Electrical Engineering, VIT University.